

MSH6 haploinsufficiency at relapse contributes to the development of thiopurine resistance in pediatric B-lymphoblastic leukemia

Nikki A. Evensen,¹ P. Pallavi Madhusoodhan,¹ Julia Meyer,² Jason Saliba,¹ Ashfiyah Chowdhury,¹ David J. Araten,³ Jacob Nersting,⁴ Teena Bhatla,¹ Tiffany L. Vincent,⁵ David Teachey,⁵ Stephen P. Hunger,⁵ Jun Yang,⁶ Kjeld Schmiegelow⁴ and William L. Carroll¹

¹Departments of Pediatrics and Pathology, Perlmutter Cancer Center, NYU-Langone Medical Center, New York, NY, USA; ²Huntsman Cancer Institute, University of Utah Medical Center, Salt Lake City, USA; ³Department of Medicine, Perlmutter Cancer Center, NYU-Langone Medical Center, New York NY, USA; ⁴Department of Pediatrics and Adolescent Medicine, The University Hospital Rigshospitalet, Copenhagen, Denmark; ⁵Department of Pediatrics and the Center for Childhood Cancer Research, Children's Hospital of Philadelphia and The Perelman School of Medicine at The University of Pennsylvania, Philadelphia, PA, USA and ⁶St. Jude Children's Research Hospital, Memphis, TN, USA

©2018 Ferrata Storti Foundation. This is an open-access paper. doi:10.3324/haematol.2017.176362

Received: July 13, 2017.

Accepted: February 7, 2018.

Pre-published: February 15, 2018.

Correspondence: william.carroll@nyumc.org

Supplemental Materials and Methods

Drug Preparation

Stock solutions of Doxorubicin (Dox) and cytarabine (Ara-c) (Sigma-Aldrich, St. Louis, MO) were prepared in double-distilled water, Prednisolone (Pred) (Pharmacia, St. Paul, MN) in 0.9% NaCl, 6-Thioguanine (6-TG) and 6-mercaptopurine (6-MP) in 0.1M NaOH, and methotrexate (MTX) (Sigma-Aldrich) in NH₄OH. Drugs were diluted in RMPI and then added to cell culture media at indicated concentrations.

Viral Preparation

HEK293T cells were transfected with pLKO.1 lentivirus constructs and packaging plasmids coding for VSV-G, Gag-pol, and Rev using lipofectamine 2000 (Invitrogen, Carlsbad, CA). Viral supernatant was used to infect cell lines along with 6 µg/ml Polybrene (Millipore, Darmstadt, Germany). After 72 hours, infected cell lines were selected with 1.5-3 µg/ml of Puromycin. Lentiviral constructs were purchased from Sigma-Aldrich: MSH6 shRNA1 TRCN0000078543, shRNA2 TRCN0000293881, control non-mammalian targeting shRNA (NT) SHC016.

Immunoblotting

Briefly, cells were lysed in RIPA buffer (50mM Tris-HCl pH7.4, 150mM NaCl 1% NP40, 0.25% Na-deoxycholate and 1X complete protease inhibitor cocktail (Sigma)). Protein was quantified using Bio-Rad DC protein assay kit and then used for immunoblotting. Primary antibodies included: MSH6 (M2445; Sigma-Aldrich), MSH2 (ab92473; Abcam, Cambridge, MA), MLH1 (ab92312; Abcam), PMS2 (ab110638; Abcam), Tubulin (ab6046; Abcam), phospho-Chk1 (317) (2344s; Cell Signaling Technology, Danvers, MA), pan-Chk1 (2360s; Cell Signaling Technology), phospho-Histone H2AX (Ser139) (γH2AX) (2577S; Cell Signaling Technology), total H2AX (2595S, Cell Signaling Technology), p53 (OP43; Millipore), and

Phospho-p53 (Ser15) (9284S, Cell Signaling Technology). Secondary antibodies used were either horseradish peroxidase-conjugated anti-mouse (NA934V) and anti-rabbit (NA931V, GE Healthcare, Piscataway, NJ, USA), or IRDye® anti-Rabbit (680RD 926-68071; 800CW 926-32211) and anti-mouse (680RD 926-68070; 800CW 926-32211) (LI-COR, Lincoln NE). Signals were visualized using ECL or ECL prime (GE Healthcare) or with the Odyssey Imaging System (LI-COR).

Apoptosis Assays

After 120 hours of treatment with indicated drugs, apoptosis was determined by Annexin V-PE and 7-Amino-actinomycin D (7-AAD) staining (BD Pharmingen, San Diego, CA) followed by flow cytometry using the FACSCalibur (Becton Dickinson, Franklin Lakes, NJ, USA). Data was analyzed by FlowJo V10 software (Tree Star Inc., Ashland, OR). Live cell percentages were used to calculate the IC50s using nonlinear regression with variable slope on GraphPad Prism 7.2 (GraphPad Prism Software Inc., La Jolla, CA). Each experiment was repeated three times, each in duplicate.

Cell Cycle Assays

Cells were treated with either 6-TG or 6-MP for 120 hours. Cells were then fixed with 70% ethanol at each time point. After all time points were collected and fixed, cells were RNase treated (QIAGEN, Valencia, CA) and stained with Propidium Iodide (PI) (Invitrogen) at a final concentration of 100 μ M, and analyzed by flow cytometry using the FACSCalibur. Live cells were captured on forward/side scatter and doublets excluded by pulse area vs. width. DNA content was analyzed using FlowJo V10 software.

MSI Analysis

The MSI Analysis System is designed to co-amplify seven different markers, 5 mononucleotide repeats (BAT-25, BAT-26, NR-21, NR-24, and MONO-27) for assessing MSI, and 2 pentanucleotide repeats (Penta C & D) for sample identification. DNA was extracted using Puregene Core Kit A (QIAGEN) and quantified using Qubit 2.0 Fluorometer (Invitrogen). DNA (2 ng) was amplified using MSI 10X primer mix

and AmpliTaq Gold DNA polymerase. PCR fragments were analyzed using an ABI 3730xl Sequencer calibrated with PowerPlex® 4-Dye (Fluorescein, JOE, and TMR) Matrix Standards along with the ILS600 size standard by Genewiz (South Plainfield, NJ). For data analysis, GeneMapper® Software Version 4.0 (Applied Biosystems, Foster City, CA) was used.

Measurement of Mutation Rate

Due to the high frequency of GPI(-) variants in 697 cells, GPI(+) clones from the NT and MSH6-KD cell lines were isolated and sorted by staining with CD59-FITC (Serotec) and collecting the upper 50th percentile on a Cytomation MoFlo instrument. Cell clones were then expanded either untreated or treated with 6-TG. NT and MSH6 shRNA1 clones were treated with 0.040 µg/ml and 0.100 µg/ml, respectively, based on IC50 values determined for these particular clones. Knockdown was confirmed by western blot for individual clones (data not shown). Cells were first stained with FLAER-Alexa 488 (Pinewood), which is GPI-dependent, followed by staining with mouse antibodies specific for GPI-linked proteins, including CD48, CD52, and CD59 (Serotec), and either a secondary rabbit anti-mouse FITC conjugate (DAKO) or directly conjugated antibodies(1). Cells were analyzed by flow cytometry on a Becton Dickinson FACScan, using Cellquest and FlowJo software. Live cells were identified by forward/side scatter, exclusion of PI, and expression of HLA-class I-PE conjugated molecules (Serotec). GPI(-) variants were defined as expressing <4% of the geometric mean of the FLAER/FITC fluorescence exhibited by the GPI(+) population. The mutant frequency (f) was calculated as the number of GPI(-) events divided by the total number of live gated events, and mutation rate (μ) was calculated as f divided by cell divisions, as previously described(2).

***In Vivo* Mouse Model of Chemoresistance**

All experiments were conducted on protocols approved by the Institutional Animal Care and Use Committee and Institutional Review Board of the Children's Hospital of Philadelphia. The UOCB1 NT and MSH6 shRNA1 expressing cell lines were transduced with lentiviral vectors (UOCB1 parent: GFP-CBG; UOCB1 MSH6 KD: GFP-CBR) and then sorted to obtain pure GFP+ cells. The cells were cultured in RMPI

with 10% FBS, NEAA, NaPyruvate, pen/strep, glutamine, and HEPES. GFP expression was checked using flow cytometry and an aliquot of cells was used for western blot analysis of MSH6 expression before injection into mice. One million cells were injected via the tail vein on day 0 (20 mice total; 10 per cell line) into NSG NOD.Cg-Prkdc^{scid} Il2rg^{tm1Wjl}/SzJ mice (The Jackson Laboratory, Bar Harbor, ME). Bioluminescence imaging (BLI) was performed using an IVIS Spectrum imaging system (Perkin Elmer) on day 6 to confirm leukemic burden and animals were randomized to treatment groups (PBS vehicle or Purixan (50 mg/kg) diluted in PBS). Mice were treated Monday through Friday starting on day 7 by gavage (0.2 ml/mouse). For BLI, on days 0, 6, 13, and 17, 3 mg of luciferin was injected intraperitoneally and mice were imaged 10 minutes post injection. On the day of sacrifice, the mice were injected one by one so that the organs could be imaged. The organs were then placed into 10% neutral buffered formalin (4% paraformaldehyde). Quantification of total flux was determined by analyzing the BLI images using Living Image Software (Perkin Elmer).

References

1. Araten DJ, Sanders KJ, Anscher D, Zamechek L, Hunger SP, Ibrahim S. Leukemic blasts with the paroxysmal nocturnal hemoglobinuria phenotype in children with acute lymphoblastic leukemia. *The American journal of pathology*. 2012;181(5):1862-9.
2. Araten DJ, Golde DW, Zhang RH, Thaler HT, Gargiulo L, Notaro R, et al. A quantitative measurement of the human somatic mutation rate. *Cancer research*. 2005;65(18):8111-7.

Supplemental Figure Legends

Figure 1: *MSH6* focally deleted specifically at relapse in 4 out of 76 B-ALL patients. Chromosomal depiction of recurring relapse-specific focal deletions spanning *MSH6* in a cohort of pediatric ALL patients. Blue lines represent regions that are deleted. Each row represents an individual patient sample. Chromosomal location shown on the top and individual gene locus shown on bottom.

Figure 2: Knockdown of *MSH6* in 697 cells resulted in a significant increase in IC50s for thiopurines. Cells were treated for 5 days with either 6-TG or 6-MP and then analyzed using flow cytometry. The percentage of live cells (Annexin V and 7AAD negative cells) was used to calculate an IC50. Individual IC50s from at least three experiments were averaged and graphed using GraphPad Prism 7.2. Bars represent +/- s.d. Significance determined by unpaired t test.

Figure 3: Chemoresistance caused by *MSH6* knockdown is specific to purine analogues. (A) Knockdown of *MSH6* in 697 cells did not lead to increased resistance to Prednisolone, Doxorubicin, Cytarabine, or Methotrexate. (B) Knockdown of *MSH6* in 697 and UOCB1 cells resulted in resistance to Temozolomide (TMZ). Cells were treated for 5 days with indicated drug and then apoptotic cells were analyzed by Annexin V and 7AAD staining followed by flow cytometry. Bars represent +/- s.d.

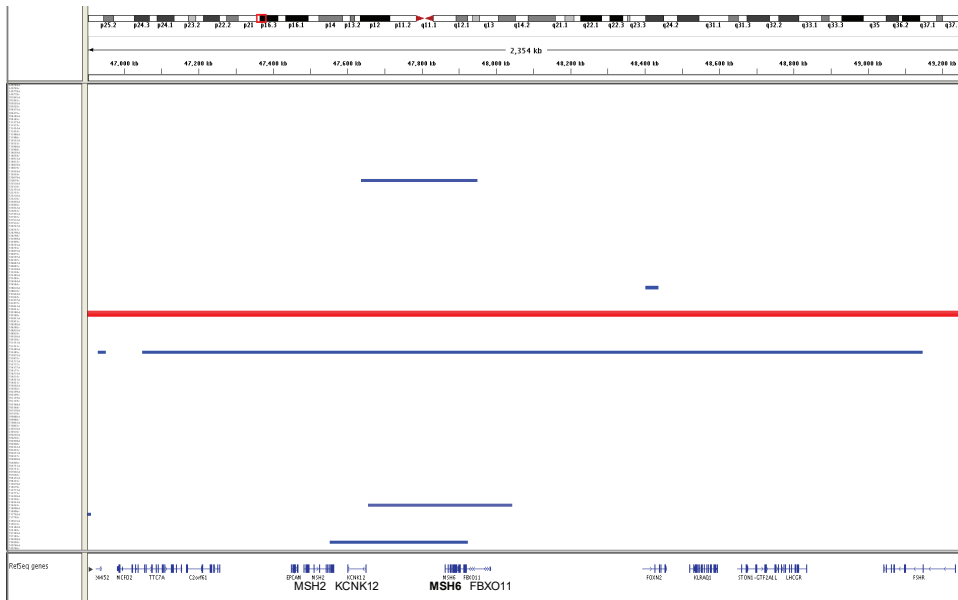
Figure 4: Knockdown of *MSH6* in UOCB1 cells resulted in a significant increase in IC50s for both 6-TG and 6-MP. Cells were treated for 5 days with either 6-TG or 6-MP and then analyzed using flow cytometry. The percentage of live cells was used to calculate an IC50. Individual IC50s from at least three experiments were averaged and graphed using GraphPad Prism 7.2. Bars represent +/- s.d. Significance determined by unpaired t test.

Figure 5: Knockdown of *MSH6* in MMR deficient Reh and RS4;11 cells did not result in a significant increase in IC50s for thiopurines. Cells were treated for 5 days with either 6-TG or 6-MP and then analyzed using flow cytometry. The percentage of live cells was used to calculate an IC50. Individual IC50s

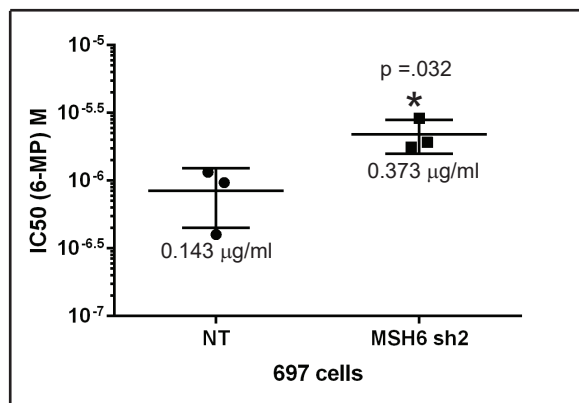
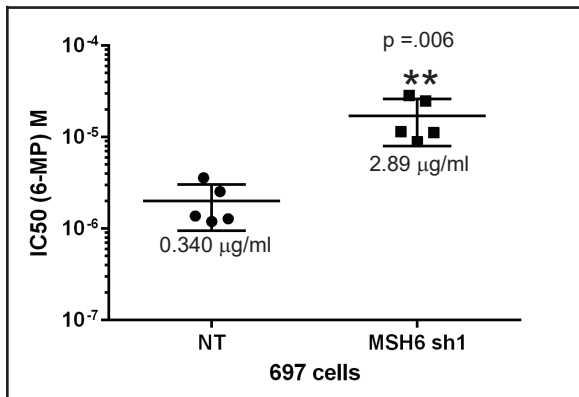
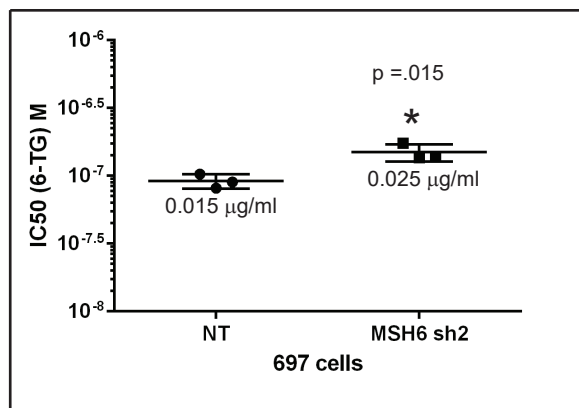
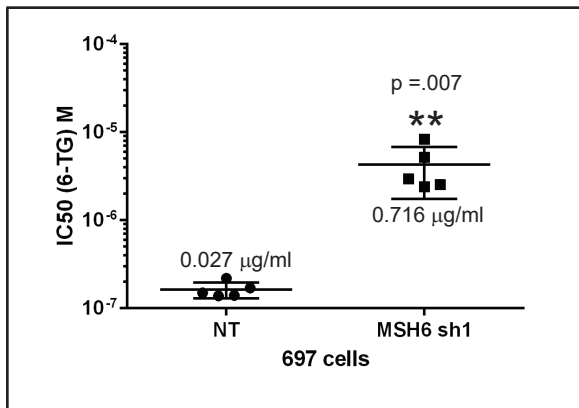
from at least two experiments were averaged and graphed using GraphPad Prism 7.2. Bars represent +/- s.d. Significance determined by unpaired t test.

Figure 6: Knockdown of MSH6 abrogated S phase arrested caused by thiopurine treatment. (A) 697 cells were treated with either 6-TG or 6-MP for a total of 5 days. Cells were fixed and stained with Propidium Iodide and analyzed for DNA content. Cell cycle analysis was performed using Flowjo V10 software using cell cycle analysis tool. Cell count histograms with the cell cycle analysis are shown for one representative experiment. (B) Cell cycle arrest was abrogated at a higher concentration of 6-TG in 697 MSH6 shRNA1 cells compared to NT cells as well as in MMR deficient Reh cells regardless of the expression of MSH6.

Supplemental Figure 1: Relapse specific, heterozygous deletion of MSH6 in 4 B-ALL patients

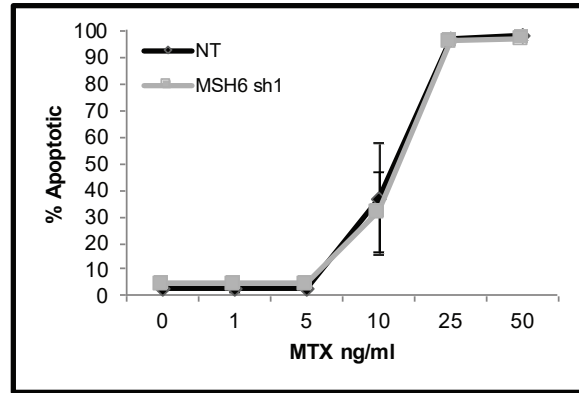
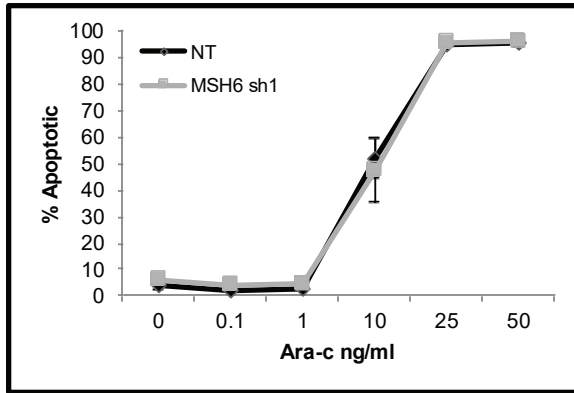
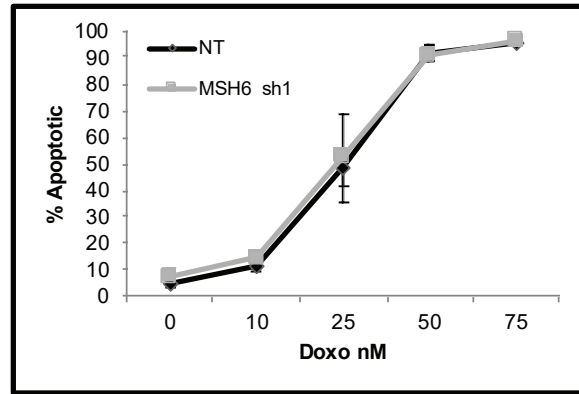
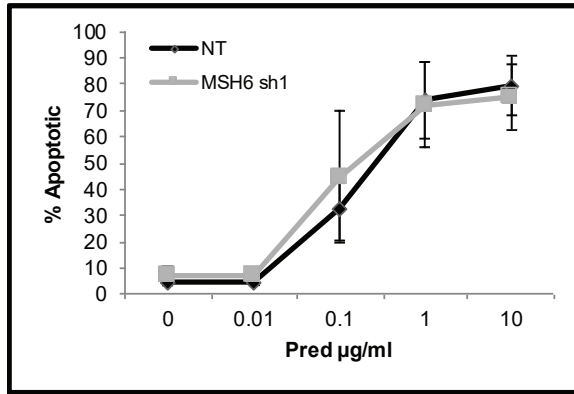


Supplemental Figure 2: Knockdown of MSH6 in 697 cells leads to thiopurine resistance.

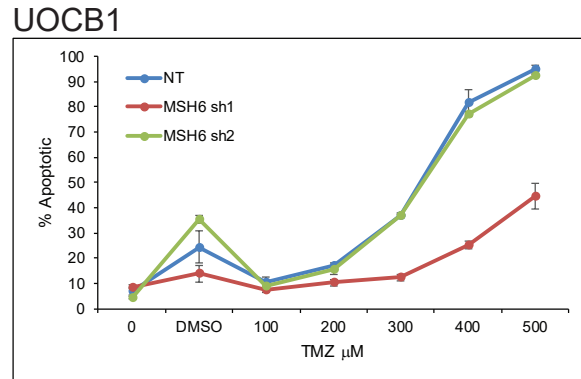
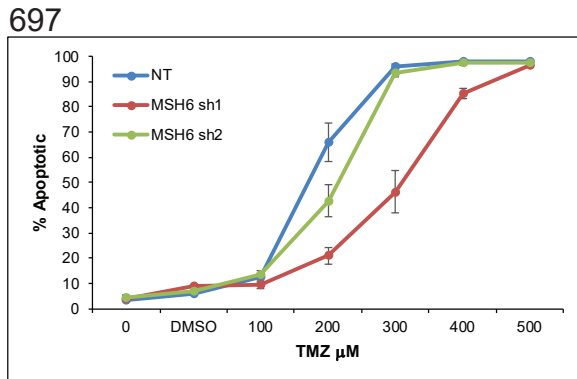


Supplemental Figure 3: Knockdown of MSH6 in 697 cells does not cause resistance to other chemotherapies used for ALL.

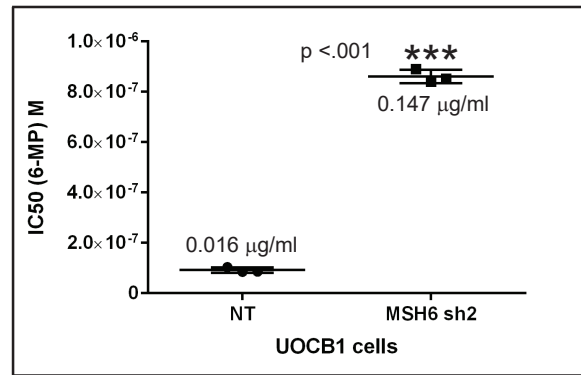
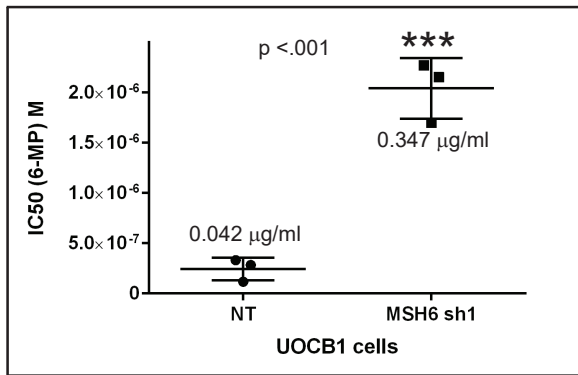
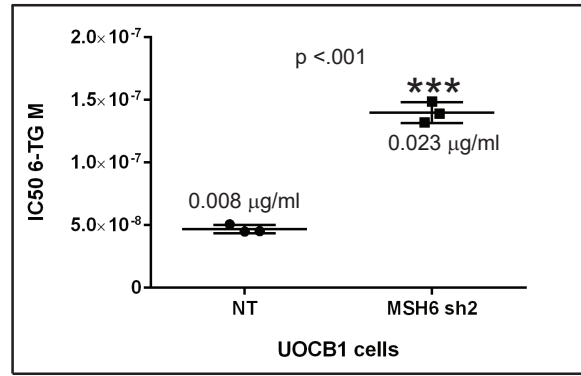
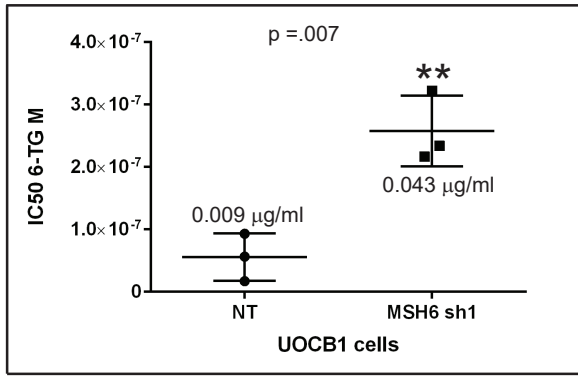
A)



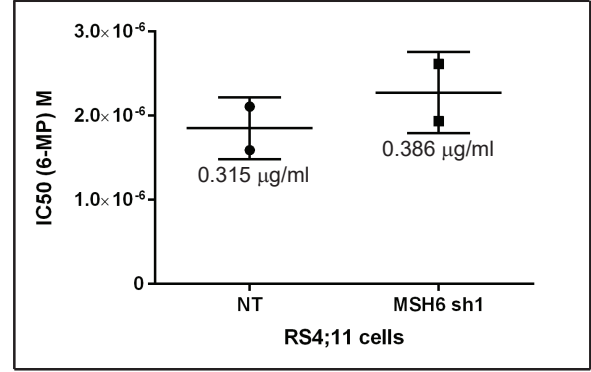
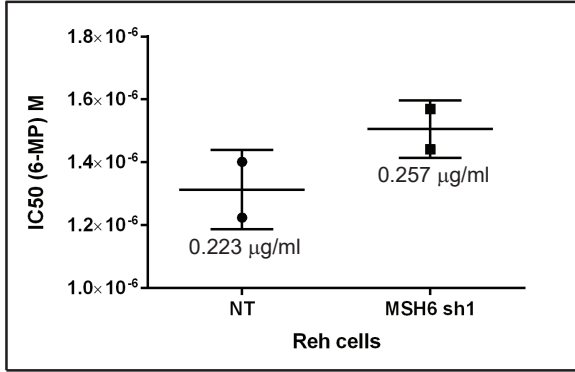
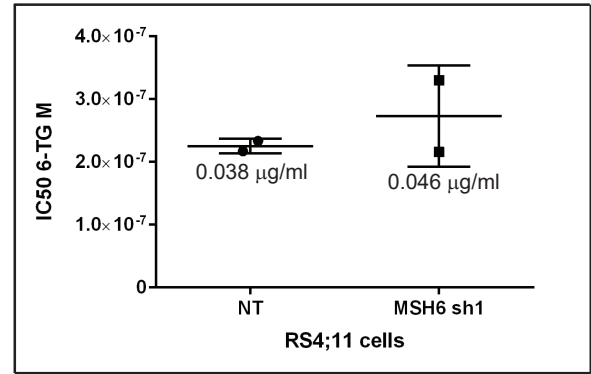
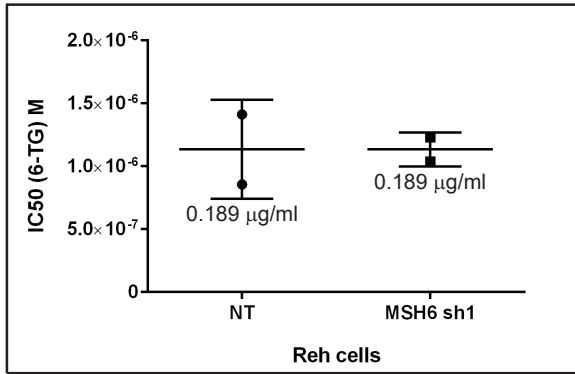
B)



Supplemental Figure 4: Knockdown of MSH6 in UOCB1 cells leads to thiopurine resistance.

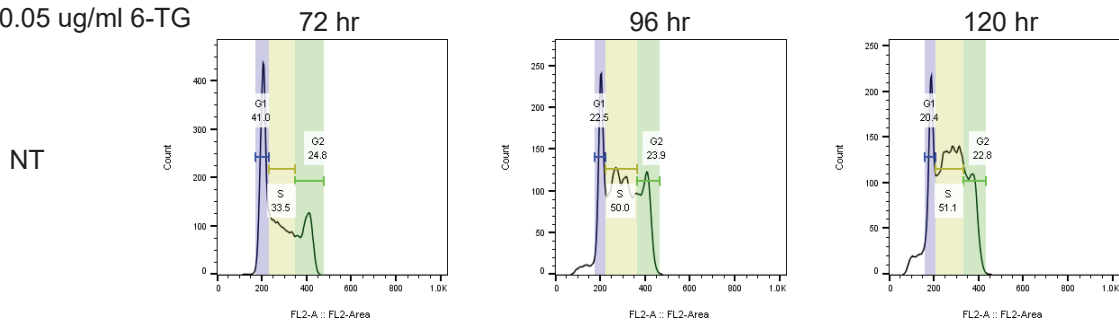


Supplemental Figure 5: Knockdown of MSH6 in MMR deficient cells lines does not lead to resistance



Supplemental Figure 6a: Knockdown of MSH6 in 697 cells disrupts thiopurine induced cell cycle arrest

0.05 ug/ml 6-TG

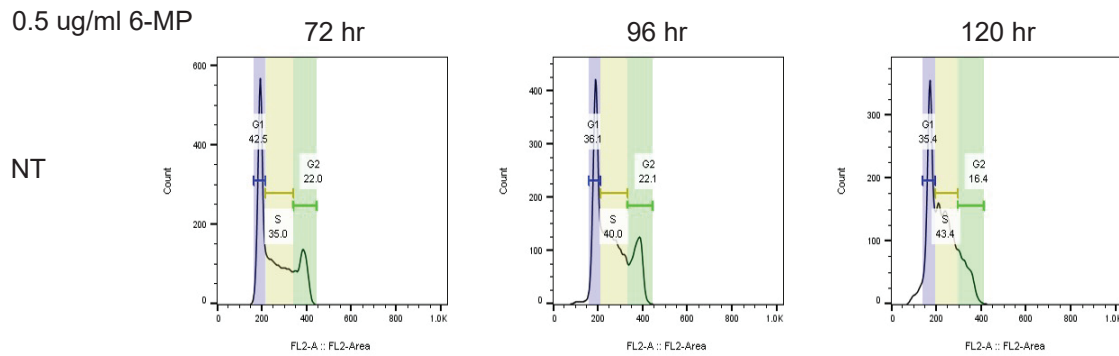


NT

MSH6 sh1

MSH6 sh2

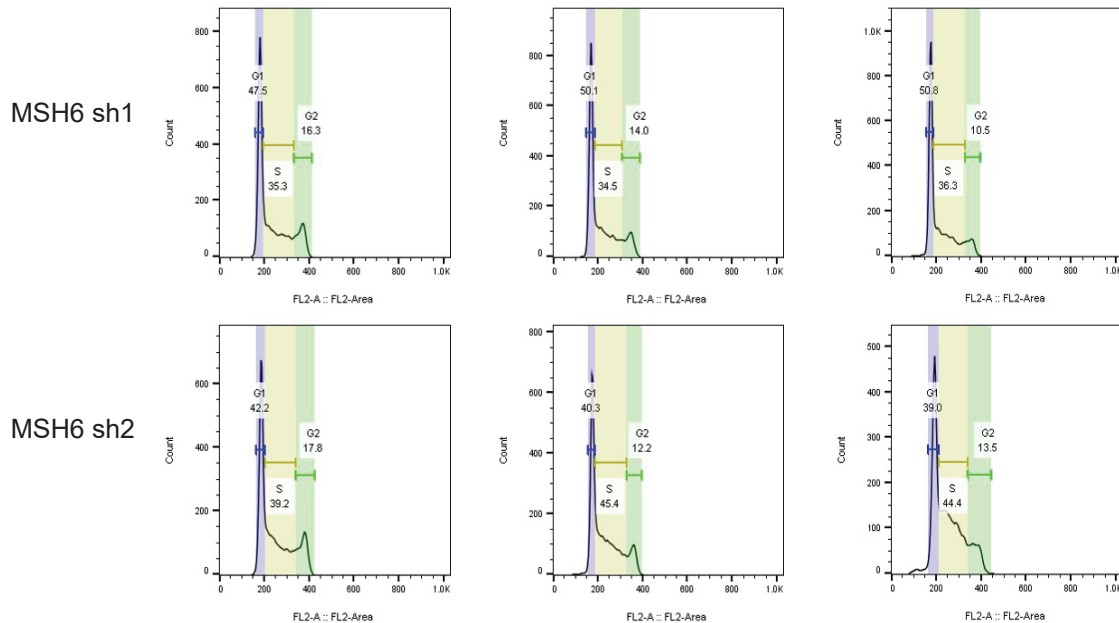
0.5 ug/ml 6-MP



NT

MSH6 sh1

MSH6 sh2



Supplemental Figure 6b: Knockdown of MSH6 in MMR proficient, but not deficient cells disrupts thiopurine induced cell cycle arrest

